Available *online* at: http://ajeeet.ft.unand.ac.id/

Andalas Journal of Electrical and Electronic Engineering Technology

ISSN 2777-0079

Analyzing Tensile Testing and Humidity Effects on Polyvinyl Alcohol, Polypyrrole Composites for Strain Sensing

Syukri Yunus [1], Rifqi Rafif[1], Aulia Aulia [1], Mohammad Hafizi Ahmad [2]

[1] *Department Electrical, Engineering Faculty, Universitas Andalas, 25163 Padang, West Sumatera, Indonesia*
[2] *Faculty of Electrical Engineering (FKE), University Technology Malaysia, 25163 Johor, Malaysia*

ARTICLE INFORMATION

Received: February 9, 2024
Revised: May 11, 2024
Accepted: June 23, 2024
Available online: July 23, 2024

KEYWORDS

Composite, Current Density, Polypyrrole, Polyvinyl Alcohol, Specific Capacitance

CORRESPONDENCE

E-mail: syukriyunus@eng.unand.ac.id

A B S T R A C T

Biocomposite strain sensors must enhance their electrical properties and understand the impact of humidity on these properties. This study aimed to enhance the current density and specific capacitance of polyvinyl alcohol (PVA) and polypyrrole (Ppy) composite materials for strain sensors. The materials were prepared by blending polyvinyl alcohol and polypyrrole, followed by magnetic stirring, drying, and stretching. Current density and specific capacitance measurements were taken before and after stretching and at three distinct relative humidity levels (50%, 75%, and 93%). After the tensile test, the results indicated a significant increase in current density by 128.46% and a corresponding rise in specific capacitance by 112.57%. Furthermore, with an increase in relative humidity from 50% to 75%, current density and specific capacitance exhibited remarkable growth of 445.95% and 899.44%, respectively. The subsequent shift from 75% to 93% relative humidity resulted in a comparatively lower percentage increase in current density and specific capacitance at 22.59% and 10.29%, respectively, due to a decrease in hydroxyl bonds. These findings align with the material's characteristic tests, confirming that the improved electrical properties can be attributed to a more uniform distribution of polypyrrole during the stretching process and increased hydroxyl bonds associated with higher humidity levels. As electrical properties increase, the sensor's sensitivity will also rise.

INTRODUCTION

Strain sensors are vital in biomedical electronics, monitoring physiological signals like heart rate, vocal cord vibrations, blinking, and subtle movements. The burgeoning interest in flexible electronic devices has prompted research into using composite materials for strain sensors. To enhance their sensitivity, it's imperative to improve the electrical properties of these sensors [1].

Composite materials are undergoing extensive development, offering the advantage of creating new mechanical properties without compromising their original attributes [2]. PVA is a synthetic polymer produced through vinyl acetate hydrolysis with alcohol and has been chosen as a composite matrix. Its advantages include mass production feasibility and a high tensile strength of up to 40.46 MPa, indicating excellent mechanical properties [3]. However, PVA exhibits low conductivity, falling into the insulator category with a range of 2.6 to 3.2 x 10-7 S/cm [5]. This limitation can be addressed by combining PVA with materials having superior electrical properties, such as conductive polymers.

Conductive polymers, often developed for energy storage devices, offer remarkable advantages, with polypyrrole (Ppy) being a widely used example. Ppy boasts easy synthesis, environmental stability, and high electrical conductivity, approaching metallic conductivity levels in the 1 to 1000 S/cm [7].

Combining PVA's robust mechanical properties with Ppy's exceptional electrical characteristics enables the creation of a composite with favorable electrical properties [9]. Numerous researchers have explored the PVA/Ppy composite through tensile strength tests, resistivity measurements, and structural analysis [10] [11].

PVA's elasticity and resistance to brittleness become apparent during tensile testing. When subjected to an applied force, deformation or strain occurs, which reverses upon load removal [12]. This strain, observed during tensile testing, evaluates changes in capacitance and current density. Moreover, it helps determine the composite's strength, with the expectation that specific capacitance and current density remain consistent throughout this process.

PVA-based composites are characterized by their hydrophilic nature, making them susceptible to water absorption and humidity sensitivity. Humidity can significantly impact the electrical properties of the composite, as water contains hydroxyl ions that

https://doi.org/10.25077/ajeeet.v4i1.91

facilitate electrical conduction [13]. Consequently, specific capacitance and current density measurements were conducted on the PVA/Ppy composite under varying humidity levels to assess their effects.

In this study, tensile tests and humidity variations were employed to evaluate their impact on the specific capacitance and current density of the PVA/Ppy composite.

METHOD

The research employed a range of equipment, including a digital scale, Petri dishes, pipettes, glassware, a hot plate magnetic stirrer, a vacuum oven, a hygrometer, a multimeter, a tensile testing machine, X-ray diffraction (XRD) testing instrument, Scanning Electron Microscopy (SEM) testing instrument, and a Fourier Transform Infra-Red (FTIR) testing instrument. The materials used in the research comprised Polyvinyl Alcohol (PVA), Polypyrrole, deionized water, and FeCl3.

Strain Sensor

Strain sensors are devices designed to convert external mechanical stimuli into electrical signals. Typically, these sensors consist of an active sensing material mounted on a flexible and stretchable supporting substrate. Strain sensors find wide-ranging applications across multiple fields, including healthcare for human motion detection, human-machine interfaces, robotics, and more [14]. In this study, PVA and Ppy were chosen as the sensor materials. PVA gave the composite stretching capabilities, while Ppy contributed to its electrical properties.

Composite Manufacturing Process

Fabricating the PVA/Ppy composite material commences with preparing the PVA solution. A hot plate magnetic stirrer dissolves 10 grams of PVA powder in 200 ml of distilled water. The mixture is stirred at 500 rpm at 80°C until the PVA solution becomes gelatinous [15]. Subsequently, the gelatinous PVA solution is blended with Ppy and FeCl3 as the initiator. The mixing occurs at 500 rpm using a hot plate magnetic stirrer for 180 minutes without additional heating. The mixed PVA and Ppy solution is then poured into 10 cm diameter Petri dishes, each containing 25 grams of the solution. These Petri dishes undergo drying in a vacuum oven at 50°C for 20 hours until they form a solid material [15].

Electrical Properties Test

Current Density

The Cyclic Voltammetry (CV) method is employed to measure current density. This method generates a voltage response that represents the current density value, determined by the movement of ions within the electrode [16]. Current density is calculated using the following formula:

$$J = \frac{I}{A} \quad (1)$$

Specific Capacitance

Specific capacitance is a characteristic of a capacitor, which refers to the ability of a material to store electrical energy in the form of electric charge [17].

$$Csp = \frac{(Ic - Id)}{(sxm)} \quad (2)$$

Characteristic Test

X-ray diffraction (XRD)

X-ray diffraction (XRD) is a technique used to analyze solid materials' crystal structure and size. Its primary purpose is to characterize the structure of the composite and assess the degree of crystallinity [18]. An XRD result graph analysis is typically performed to examine crystallinity. One common approach is the deconvolution method, carried out using ORIGIN PRO software, which aids in identifying and quantifying the peaks on the XRD graph [19]. The crystallinity index of a material can be calculated using the following equation:

$$CI(\%) = \frac{Sc}{St} \times 100 \quad (3)$$

Scanning Electron Microscope (SEM)

Scanning Electron Microscopy (SEM) is a valuable technique used for characterizing the microstructure of materials. It enables the detailed observation of a material's morphology, texture, crystal characteristics, and composition on the surface of individual grains [20]. SEM closely examines particle shape, size, and arrangement within the material under investigation.

Fourier Transform Infra-Red (FTIR)

Fourier Transform Infrared (FTIR) is a versatile technique employed to detect functional groups, identify compounds, and generate infrared spectra by analyzing absorbance, emission, photoconductivity, or Raman scattering. This approach can be applied to various sample types, including solids, liquids, and gases [21].

RESULTS AND DISCUSSION

Material Manufacturing Results

In the preparation of PVA/Ppy composite materials, several circular thin material samples were produced. Each sample has a diameter of 10 cm and a thickness of 0.02 cm. In naming the samples, there are two types of samples to be discussed: WTT (Without Tensile Test) samples and TT (Tensile Test) samples. Later, these samples will undergo tensile test treatment to see the response. Figure 1 shows the result of making the PVA/Ppy composite material.

Figure 1 PVA/Ppy Composite Material Sample

Tensile Test Results

After conducting the tensile test on the TT sample, the obtained graph is shown in Figure 2. Based on the tensile test results, it is found that the TT sample has a stress of 22.27 MPa and a strain of 0.25. Previous research results state that this PVA/Ppy

composite has a tensile strength of up to 40.46 MPa, indicating good mechanical properties [4]. The material's elastic modulus can be calculated as 89.08 MPa, indicating its elastic nature, where the material can return to its original shape after being subjected to a force [22].

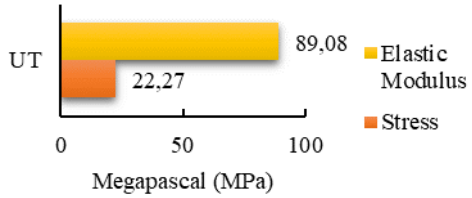

Figure 1 Tensile Test Diagram of TT Sample

Humidity Conditioning Results

In this study, humidity conditioning of the samples was conducted using an airtight box. The samples were placed inside the box, and the humidity was controlled using silica gel. The amount of silica gel used was adjusted to achieve the desired humidity level. A hygrometer was used to monitor the humidity inside the box, which provided relative humidity (RH) values. The humidity values inside the box were conditioned at levels of 50% RH, 75% RH, and 93% RH.

Current Density Results

In cyclic voltammetry (CV) testing, current density measurements are conducted to obtain information about the composite material's current density and specific capacitance values. This test was carried out with a sample with an area of 2 cm^2 and a mass of 0.028 gr. The testing is performed by varying the voltage from 1000 mV to 1500 mV using a 1 M H2SO4 electrolyte solution. The reference electrode is Ag/AgCl, while the auxiliary is platinum (Pt). The results of the CV testing on the WTT and TT samples, as well as the humidity variations, can be found in Figure 3.

In Figure 3, a voltammogram curve is observed, indicating the occurrence of reduction-oxidation reactions. The curve shows the charge current (Ic), which represents the current during the oxidation peak, and the discharge current (Id), which represents the current during the reduction peak [23].

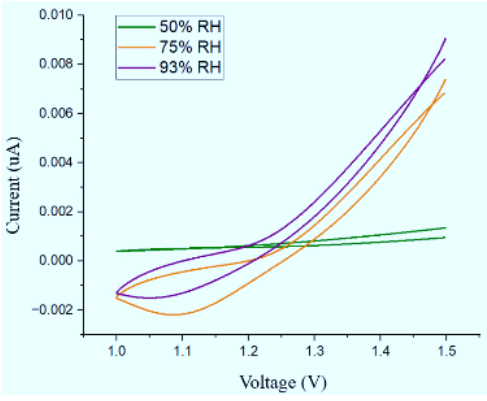

(a)

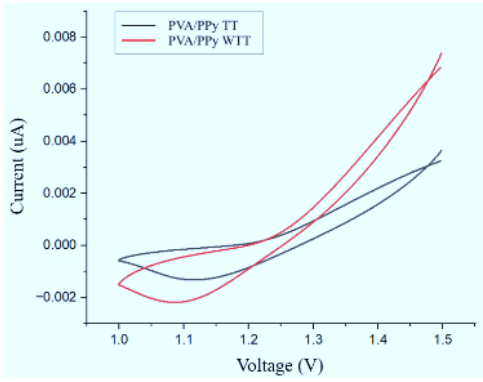

(b)

Figure 3 Voltammogram Graph of PVA/Ppy(a) with and without tensile (b) several variations humidity

Based on Figure 4, it can be observed that the current density increases after the pulling process and with an increase in humidity in the composite. In the testing of the TT sample, the current density increased by 128.46% compared to the WTT sample. The increase in current density in the composite material is attributed to the elastic properties of PVA. When the composite material is stretched, the flexible nature of PVA allows the PVA structure to elongate, enhancing the Ppy absorption within the PVA. As a result, the current density of the composite material increases [24].

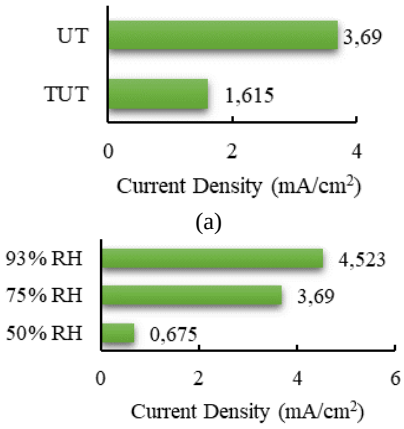

(a)

(b)

Figure 4 Current Density Results, (a) Tensile Test Variation, (b) Humidity Variation

In the humidity variation sample, the increase in current density from 50% to 75% RH is 445.95%, while from 75% to 93% RH is 22.59%. The decrease in the increase from 75% to 93% RH is due to a lower number of bound hydroxyl groups, as many hydroxyl groups are already bonded during the increase from 50% to 75% RH. Water is a substance that can ionize into hydrogen ions and hydroxide ions, making it a weak electrolyte. The electrolyte is substances that can dissociate into ions when dissolved in water and conduct electric current. These ions act as charge carriers that enable the flow of electric current. Therefore, higher humidity and stretching in the composite result in higher current density.

Specific Capacitance Results

The specific capacitance is calculated based on the data obtained from the CV testing. Figure 5 shows the results of specific

 https://doi.org/10.25077/ajeeet.v4i1.91

capacitance testing on samples with different tensile variations. The specific capacitance value in the TT sample increased by 112.57% compared to the WTT sample. The humidity variation testing from 50% to 75% RH resulted in a specific capacitance increase of 899.44%, while from 75% to 93% RH, it experienced an increase of 10.29%. The test results indicate that the samples' specific capacitance value increases with tensile variations and humidity changes. This increase in specific capacitance is because, during the pulling process, Ppy becomes more integrated with PVA, and higher humidity levels increase the binding of hydroxyl groups in the composite [25] [26].

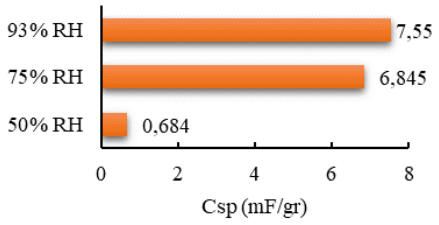

(a)

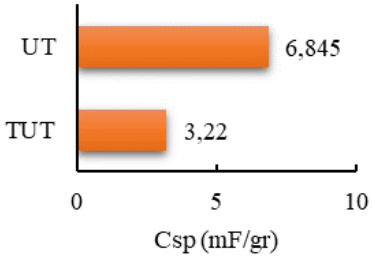

(b)

Figure 5 Specific Capacitance Results, (a) Tensile Test Variation, (b) Humidity Variation

Characteristic Test Results

SEM Results and Discussion

SEM analysis was performed at a magnification of 10,000 times, as depicted in Figure 6, which shows the morphological structures of the WTT and TT samples. In the WTT sample, the morphological structure reveals the amalgamation of PVA and Ppy composite materials, though the Ppy density remains imperceptible. Conversely, in the TT sample, the morphological structure illustrates a more intimate adherence of Ppy to PVA, facilitating greater Ppy accessibility. These SEM findings align with the previously conducted electrical property tests, as the enhanced adhesion of Ppy in the composite material bolsters its electrical properties due to Ppy's high conductivity [27].

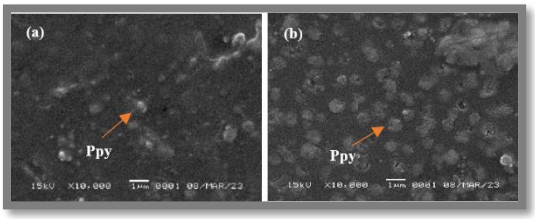

Figure 6 SEM Test Results, (a) WTT Sample, (b) TT Sample

Figure 7 illustrates the morphological structure of samples with controlled humidity variations. In the sample with 50% RH humidity, it can be observed that Ppy has not fully dispersed within the PVA. In the sample with 75% RH humidity, Ppy starts to spread within the composite material, and PVA also binds to hydroxyl groups to a greater extent. Meanwhile, in the sample with 93% RH humidity, there is an increase in the number of hydroxyl groups binding to PVA, resulting in a more even distribution of Ppy in the composite material. Increased humidity causes PVA to bind with more hydroxyl groups and undergo stretching, allowing Ppy to spread within the sample.

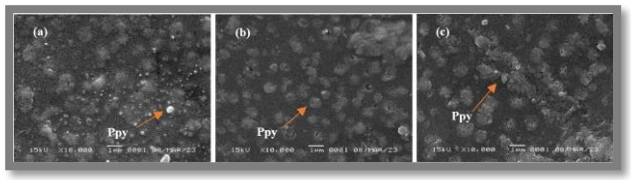

Figure 7 SEM Test Results, (a) 50%RH Sample, (b) 75%RH Sample, (c) 93%RH Sample

XRD Results and Discussion

XRD (X-ray Diffraction) analysis was employed to investigate the crystal structure of the PVA/Ppy composite material. Figures 10 and 11 display the XRD graphs resulting from the testing. Within the XRD graph, distinctive peaks emerge at angles ($18 < 2\theta < 20$) indicative of PVA's semi-crystalline nature [28]. However, the XRD pattern of the composite material exhibits an amorphous structure, evidenced by a decrease in the intensity of the PVA diffraction peak following tensile testing [29]. This amorphous structure can be attributed to the influence of tensile testing on intermolecular interactions between PVA/Ppy chains, reducing the composite material's degree of crystallinity.

To quantify the crystallinity of the samples subjected to various tensile and humidity conditions in this study, deconvolution was employed. The deconvolution method leveraged ORIGIN PRO software to collect the necessary data for crystallinity calculations [19].

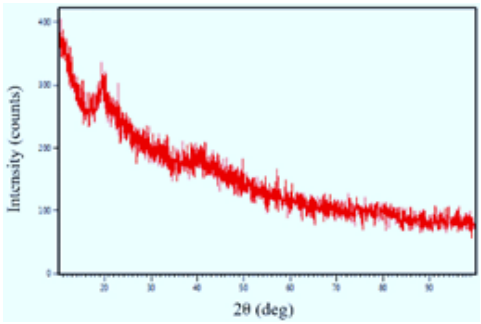

(a)

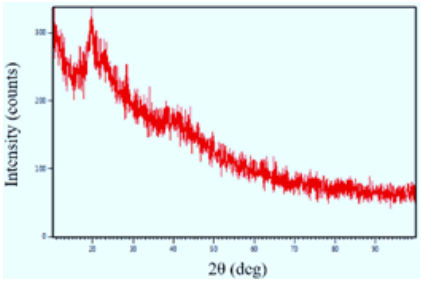

(b)

Figure 8 XRD graphs of (a) WTT sample, (b) TT sample

In the case of the WTT (without tensile testing) sample, the determined crystallinity is 10.45%, whereas the TT (tensile tested) sample exhibits a crystallinity of 5.7%. The decline in crystallinity observed in the TT sample can be attributed to the increased spacing of intermolecular interactions between PVA/Ppy chains following tensile testing. It is important to note that the sample's electrical properties depend on the number of charge carriers and their mobility within the material [29].

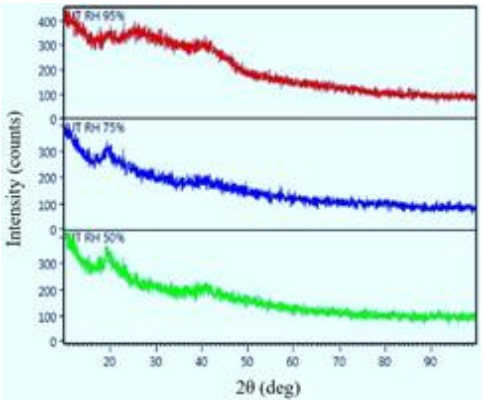

Figure 9 XRD Graph of Humidity Variation

.Based on the XRD calculations, the obtained crystallinity results for samples at 50% RH, 75% RH, and 93% RH are 10,12%, 5,7%, and 3,47%, respectively. The decrease in crystallinity in these samples is attributed to the hydrophilic nature of PVA. When PVA absorbs water molecules, the PVA structure expands, increasing the distance between conductive filler particles within the composite. Therefore, high humidity can enhance the conductivity of the composite [30].

FTIR Results and Discussion

In the FTIR characterization test, the WTT and TT samples were analyzed to observe the functional groups present in both of them. The FTIR spectra of both samples can be seen in Figure 10. The FTIR results indicate that both samples exhibit the same pattern, suggesting that the variations in the tensile test did not lead to the formation of new functional groups. However, the peak positions and intensities of the OH functional groups changed. In the FTIR spectrum within the range of 3500 - 3100, absorptions from the hydroxyl (OH) functional groups can be observed in the WTT and TT samples. However, in the TT sample, the transmittance is lower compared to the WTT sample, indicating a stronger peak intensity in that region. Stretching after the sample was subjected to tension allowed more hydroxyl groups to bond within the sample [31].

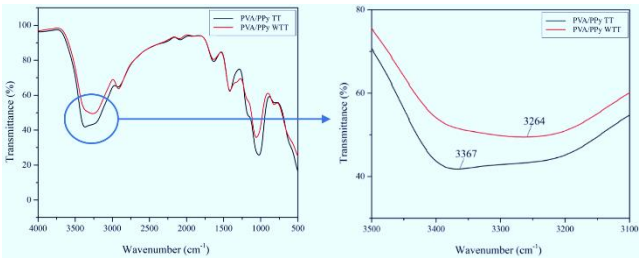

Figure 10 FTIR Spectrum of Tensile Test Variation

In the FTIR characterization test, various samples of the PVA/Ppy composite material, each having different humidity levels, were analysed to discern the functional groups present in each sample. Figure 11 displays the FTIR spectra for the samples with varying humidity levels. These spectra reveal similar patterns in both samples.

We focused on the FTIR spectrum within the 3500 - 3100 range to examine the absorption attributed to the hydroxyl (OH) functional groups. Notably, in the sample subjected to 93% humidity, we observed lower transmittance than the samples exposed to 75% and 50% humidity. This lower transmittance indicates a more pronounced peak intensity in that region compared to the samples exposed to 75% and 50% humidity. These findings reflect the increased water absorption in the sample with 93% humidity [32].

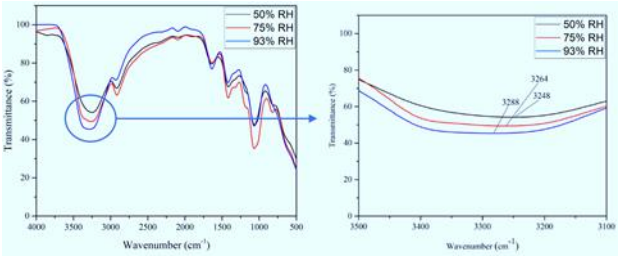

Figure 11 FTIR Spectrum of Humidity Variation

CONCLUSIONS

Based on the research findings, it is evident that the tensile test positively impacted the PVA/Ppy composite, resulting in increased current density and specific capacitance. This enhancement can be attributed to the increased accessibility of Ppy within PVA due to stretching, leading to the formation of voids in PVA. Additionally, the influence of humidity on the composite material further augments the current density and specific capacitance by increasing the hydroxyl groups within the composite material.

The results from characterizing the composite materials using FTIR, XRD, and SEM confirm the effects of tensile and humidity testing on PVA/Ppy composites. Notably, the samples subjected to tensile testing and exposed to higher humidity exhibited a greater presence of hydroxyl groups. Furthermore, the level of crystallinity within the composite material decreased following the tensile and high humidity tests. The structure of Ppy within the composite also exhibited a more uniform distribution due to the rigorous tensile and humidity testing.

In light of these findings, the PVA/Ppy composite emerges as a promising material for fabricating strain sensors, showcasing high sensitivity and the ability to detect subtle movements.

ACKNOWLEDGMENT

The researcher would like to thank colleagues who have helped complete this research. In particular, the authors would like to thank the Department of Electrical Engineering and the Faculty of Engineering, Universitas Andalas, who have assisted in funding this research.

REFERENCES

[1] W. Shi, G. Han, Y. Chang, H. Song, W. Hou, and Q. Chen, "Using Stretchable PPy@PVA Composites as a High-Sensitivity Strain Sensor to Monitor Minute Motion," *ACS Appl. Mater. Interfaces*, vol. 12, no. 40, pp. 45373–45382, 2020, doi: 10.1021/acsami.0c14503.

[2] M. Yani, B. Suroso, and R. Rajali, "Mechanical Properties Komposit Limbah Plastik," *J. Rekayasa Mater. Manufaktur dan Energi*, vol. 2, no. 1, pp. 74–83, 2019, doi: 10.30596/rmme.v2i1.3071.

[3] D. Qureshi *et al.*, "Fabrication and characterization of poly (Vinyl alcohol) and chitosan oligosaccharide-based blend materials," *Gels*, vol. 7, no. 2, pp. 1–23, 2021, doi: 10.3390/gels7020055.

[4] N. V Bhat, A. P. Gadre, and V. A. Bambole, "Structural , Mechanical , and Electrical Properties of," no. August 2000, pp. 2511–2517, 2001.

[5] M. J. Simanjuntak, "Studi Material Polivinil Alkohol (PVA) Di Modifikasi dengan Acrylamide (Aam) Sebagai Material Sensitif Terhadap Kelembaban," *Thesis*, p. Depok: Universitas Indonesia, 2008.

[6] B. susanto Widodo, Harlia, and I. Syahbanu, "Sintesis Komposit Polimer Konduktif Polipirol (PPy)/ Selulosa Bakteri," *Jkk*, vol. 7, no. 1, pp. 59–65, 2018.

[7] J. H. Min, M. Patel, and W. G. Koh, "Incorporation of conductive materials into hydrogels for tissue engineering applications," *Polymers (Basel).*, vol. 10, no. 10, pp. 1–36, 2018, doi: 10.3390/polym10101078.

[8] A. Batool, F. Kanwal, M. Imran, T. Jamil, and S. A. Siddiqi, "Synthesis of polypyrrole/zinc oxide composites and study of their structural, thermal and electrical properties," *Synth. Met.*, vol. 161, no. 23–24, pp. 2753–2758, 2012, doi: 10.1016/j.synthmet.2011.10.016.

[9] S. E. Lindsey and G. B. Street, "Conductive composites from polyvinyl alcohol and polypyrrole," *Synth. Met.*, vol. 10, no. 1, pp. 67–69, 1984, doi: 10.1016/0379-6779(84)90080-8.

[10] S. Yunus, A. Yusman, M. Mahardika, H. Abral, and R. Nazir, "Increasing Electrical Conductivity of Bacterial Cellulose/Polypyrrole Bio Composite Materials Prepared Using the Pulling Technique," *TEM J.*, vol. 12, no. 1, pp. 370–376, 2023, doi: 10.18421/TEM121-46.

[11] S. W. Tsai and H. T. Hahn, *Introduction to Composite Materials*. 2018.

[12] M. Muchiar and K. Mahmud, "Penelitian Terhadap Deformasi Pada Paduan Aluminium Tipe a5083P-O Dengan Teknik Interferometri Optik," *J. Teknol.*, vol. 8, no. 2, p. 85, 2016, doi: 10.24853/jurtek.8.2.85-88.

[13] J. M. Yang, W. Y. Su, T. L. Leu, and M. C. Yang, "Evaluation of chitosan/PVA blended hydrogel membranes," *J. Memb. Sci.*, vol. 236, no. 1–2, pp. 39–51, 2004, doi: 10.1016/j.memsci.2004.02.005.

[14] H. Souri *et al.*, "Wearable and Stretchable Strain Sensors: Materials, Sensing Mechanisms, and Applications," *Adv. Intell. Syst.*, vol. 2, no. 8, p. 2000039, 2020, doi: 10.1002/aisy.202000039.

[15] H. Abral *et al.*, "Effect of ultrasonication duration of polyvinyl alcohol (PVA) gel on characterizations of PVA material," *J. Mater. Res. Technol.*, vol. 9, no. 2, pp. 2477–2486, 2020, doi: 10.1016/j.jmrt.2019.12.078.

[16] L. Bao, J. Zang, and X. Li, "Flexible Zn2SnO4/MnO2 core/shell nanocable-carbon microfiber hybrid composites for high-performance supercapacitor electrodes," *Nano Lett.*, vol. 11, no. 3, pp. 1215–1220, 2011, doi: 10.1021/nl104205s.

[17] E. Taer, Z. Zulkifli, E. N. Arif, and R. Taslim, "Analisa Kapasitansi Spesifik Elektroda Karbon Superkapasitor dari Kayu Karet Terhadap Laju Scan Berdasarkan Variasi aktivasi HNO3," *Spektra J. Fis. dan Apl.*, vol. 1, no. 1, pp. 35–40, 2016, doi: 10.21009/spektra.011.06.

[18] M. Das and D. Sarkar, "Development of room temperature ethanol sensor from polypyrrole (PPy) embedded in polyvinyl alcohol (PVA) matrix," *Polym. Bull.*, vol. 75, no. 7, pp. 3109–3125, 2018, doi: 10.1007/s00289-017-2192-y.

[19] M. Serhan *et al.*, "Ferromagnetic iron oxide-cellulose nanocomposites prepared by ultrasonication," *AIChE Annu. Meet. Conf. Proc.*, vol. 2019-Novem, no. c, pp. 1–4, 2019, doi: 10.1039/x0xx00000x.

[20] K. Akhtar, S. A. Khan, S. B. Khan, and A. M. Asiri, *Scanning electron microscopy: Principle and applications in nanomaterials characterization*. 2018.

[21] M. T. Arief Elang Raharja, Dr. Eng. Asep Suhendi, S.Si., M.Si., Dr. Dudi Darmawan, S.Si., "Resistivity Measurement on Thin Conductor Plate Using Four Point Probe Method," vol. 6, no. 2, pp. 5305–5313, 2019.

[22] R. R. H. Hau, M. Masturi, I. Yulianti, S. K. Hau, and S. D. Talu, "Modulus Elastisitas Bambu Betung Dengan Variabel Panjang," vol. V, pp. SNF2016-CIP-37-SNF2016-CIP-42, 2016, doi: 10.21009/0305020108.

[23] K. Kannan, M. Hussien, A. M. Abdullah, and K. Kumar, "Supporting Information Fabrication of ZnO-Fe-MXene based nanocomposites for efficient CO 2 reduction," pp. 0–1, 2020.

[24] Y. Li *et al.*, "Facile preparation of stretchable and self-healable conductive hydrogels based on sodium alginate/polypyrrole nanofibers for use in flexible supercapacitor and strain sensors," *Int. J. Biol. Macromol.*, vol. 172, pp. 41–54, 2021, doi: 10.1016/j.ijbiomac.2021.01.017.

[25] V. P. Anju, P. R. Jithesh, and S. K. Narayanankutty, "A novel humidity and ammonia sensor based on nanofibers/polyaniline/polyvinyl alcohol," *Sensors Actuators, A Phys.*, vol. 285, pp. 35–44, 2019, doi: 10.1016/j.sna.2018.10.037.

[26] X. Zhang, M. Gao, L. Tong, and K. Cai, "Polypyrrole/nylon membrane composite material for ultra-flexible all-solid supercapacitor," *J. Mater.*, vol. 6, no. 2, pp. 339–347, 2020, doi: 10.1016/j.jmat.2019.11.004.

[27] D. Nerkar, M. Rajwade, S. Jaware1, and M. Jog, "Synthesis and characterization of Polyvinyl Alcohol-Polypyrrole-Silver nanocomposite polymer materials with core-shell structure," *Int. J. Nano Dimens*, vol. 11, no. 3, pp. 205–214, 2020, [Online]. Available: http://creativecommons.org/licenses/by/4.0/.

[28] G. M. Elkomy, S. M. Mousa, and H. Abo Mostafa, "Structural and optical properties of pure PVA/PPY and cobalt chloride doped PVA/PPY materials," *Arab. J.*

Chem., vol. 9, pp. S1786–S1792, 2016, doi: 10.1016/j.arabjc.2012.04.037.

[29] K. M. Manikandan, A. Yelilarasi, P. Senthamaraikannan, S. S. Saravanakumar, A. Khan, and A. M. Asiri, "The conducting polymer electrolyte based on polypyrrole-polyvinyl alcohol and its application in low-cost quasi-solid-state dye-sensitized solar cells," *J. Solid State Electrochem.*, vol. 22, no. 12, pp. 3785–3797, 2018, doi: 10.1007/s10008-018-4070-4.

[30] J. Bhadra, A. Popelka, A. Abdulkareem, M. Lehocky, P. Humpolicek, and N. Al-Thani, "Effect of humidity on the electrical properties of the silver-polyaniline/polyvinyl alcohol nanocomposites," *Sensors Actuators, A Phys.*, vol. 288, pp. 47–54, 2019, doi: 10.1016/j.sna.2019.01.012.

[31] H. Abral *et al.*, "Characterization of compressed bacterial cellulose nanopaper material after exposure to dry and humid conditions," *J. Mater. Res. Technol.*, vol. 11, pp. 896–904, 2021, doi: 10.1016/j.jmrt.2021.01.057.

[32] E. Syafri *et al.*, "Synthesis and characterization of cellulose nanofibers (CNF) ramie reinforced cassava starch hybrid composites," *Int. J. Biol. Macromol.*, vol. 120, pp. 578–586, 2018, doi: 10.1016/j.ijbiomac.2018.08.134.

NOMENCLATURE

Components	Parameters
Three Phase Source	Resistance = 0.45 Ω
	Inductance = 63.73 H
	Phase Voltage = 66 kV
66/11 kV Transformer	Nominal Power = 23 MVA
	Frequency = 50 Hz
Overhead Distribution Line	Resistance = 0.2228 Ω /km
	Inductance = 84.67 µH/km
	Capacitance = 0.27724 nF/km
Underground Distribution Line	Resistance = 0.0796 Ω/km
	Inductance = 0.2833 mH/km
	Capacitance = 0.52 µF/km
11/0.433 kV Transformer	Nominal Power = 630 kVA
	Frequency = 50Hz
Load	Active Power = 262,721.79 W
	Reactive Power = 162.8 MVar